Solitons in the noisy Burgers equation

Hans C. Fogedby[1,2] and Axel Brandenburg[2]
[1]*Institute of Physics and Astronomy, University of Aarhus, DK-8000, Aarhus C, Denmark*
[2]*NORDITA, Blegdamsvej 17, DK-2100, Copenhagen Ø, Denmark*
(Received 7 May 2001; published 22 July 2002)

We investigate numerically the coupled diffusion-advective type field equations originating from the canonical phase space approach to the noisy Burgers equation or the equivalent Kardar-Parisi-Zhang equation in one spatial dimension. The equations support stable right hand and left hand solitons and in the low viscosity limit a long-lived soliton pair excitation. We find that two identical pair excitations scatter transparently subject to a size-dependent phase shift and that identical solitons scatter on a static soliton transparently without a phase shift. The soliton pair excitation and the scattering configurations are interpreted in terms of growing step and nucleation events in the interface growth profile. Finally, we show that growing steps perform an anomalous random walk with dynamic exponent $z=3/2$.

DOI: 10.1103/PhysRevE.66.016604 PACS number(s): 05.45.Yv, 05.10.Gg, 64.60.Ht

I. INTRODUCTION

There is a continuing interest in the strong coupling aspects of stochastically driven nonequilibrium systems. The phenomena in question are ubiquitous and comprise turbulence in fluids, interface, and growth problems, and chemical and biological systems. In this context the noisy Burgers equation or the equivalent Kardar-Parisi-Zhang (KPZ) equation, describing the nonequilibrium growth of a noise-driven interface, provide a simple continuum model of an open driven nonlinear system exhibiting scaling and pattern formation.

In one dimension, which is our concern here, the noisy Burgers equation for the local slope, $u(x,t)=\nabla h(x,t)$, of a growing interface has the form [1,2]

$$\frac{\partial u}{\partial t}=\nu\nabla^2 u+\lambda u\nabla u+\nabla\eta, \tag{1}$$

$$\langle\eta(x,t)\,\eta(0,0)\rangle=\Delta\,\delta(x)\,\delta(t). \tag{2}$$

The height profile (in a comoving frame) $h(x,t)$ is then governed by the equivalent KPZ equation [3,4]

$$\frac{\partial h}{\partial t}=\nu\nabla^2 h+\frac{\lambda}{2}(\nabla h)^2+\eta. \tag{3}$$

In Eqs. (1) and (3) ν is the damping or viscosity characterizing the linear diffusive term, λ a coupling strength for the nonlinear mode coupling or growth term, and η a Gaussian white noise, driving the system into a statistically stationary state. The noise is correlated according to Eq. (2) and characterized by the strength Δ. Moreover, the Burgers equation is invariant under the slope-dependent Galilean transformation

$$x\to x-\lambda u_0 t,\quad u\to u+u_0, \tag{4}$$

i.e., the interface is superimposed with a constant slope in a moving frame.

The Burgers equation (1) and its KPZ equivalent in one and higher dimensions have been the subject of intense scrutiny in recent years owing to their paradigmatic significance within the field theory of nonequilibrium systems [5–15].

In a series of papers the one-dimensional case defined by Eqs. (1) and (2) has been analyzed in an attempt to uncover the physical mechanisms underlying the pattern formation and scaling behavior. Emphasizing that the noise strength Δ constitutes the relevant nonperturbative parameter that is driving the system into a statistically stationary state, the method was initially based on a weak noise saddle point approximation to the Martin-Siggia-Rose functional formulation of the noisy Burgers equation [16–19]. This work was a continuation of earlier work based on the mapping of a solid-on-solid model onto a continuum spin model [20]. More recently the functional approach has been superseded by a *canonical phase space method* deriving from the canonical structure of the Fokker-Planck equation associated with the Burgers equation [21–27]. Below we briefly summarize these findings.

The functional or the equivalent phase space approach valid in the weak noise limit $\Delta\to 0$ replaces the stochastic Langevin-type Burgers equation (1) by coupled deterministic diffusion-advection type mean field equations,

$$\frac{\partial u}{\partial t}=\nu\nabla^2 u-\nabla^2 p+\lambda u\nabla u, \tag{5}$$

$$\frac{\partial p}{\partial t}=-\nu\nabla^2 p+\lambda u\nabla p, \tag{6}$$

for the slope $u(x,t)$ and a canonically conjugate noise field $p(x,t)$, replacing the stochastic noise η. The field equations bear the same relation to the Fokker-Planck equations as the classical equations of motion bear to the Schrödinger equation in the semiclassical WKB approximation [28].

To justify the weak noise limit we recall the analogy with the WKB approximation in quantum mechanics which, owing to its nonperturbative character, captures features like bound states and tunneling amplitudes, which are generally inaccessible to perturbation theory. Therefore, we anticipate that the present weak noise approach to the Burgers equation

also accounts correctly, at least in a qualitative sense, for the stochastic properties even at larger noise strength.

Equations (5) and (6) derive from a principle of least action characterized by an action $S(u'\to u'',t)$ associated with an orbit $u'(x)\to u''(x)$ traversed in time t [29],

$$S(u'\to u'',t)=\int_{0,u'}^{t,u''} dt\,dx\left(p\frac{\partial u}{\partial t}-\mathcal{H}\right) \tag{7}$$

with Hamiltonian density

$$\mathcal{H}=p\left(\nu\nabla^2 u+\lambda u\nabla u-\frac{1}{2}\nabla^2 p\right). \tag{8}$$

The action is of central importance and serves as a weight function for the noise-driven nonequilibrium configurations. The action, moreover, yields access to the time-dependent and stationary probability distributions,

$$P(u'\to u'',t)\propto\exp\left[-\frac{S(u'\to u'',t)}{\Delta}\right], \tag{9}$$

$$P_{\rm st}(u'')=\lim_{t\to\infty}P(u'\to u'',t), \tag{10}$$

and associated moments, e.g., the stationary slope correlations

$$\langle u(x,t)u(0,0)\rangle=\int\prod du\;\; u''(x)u'(0)\times P(u'\to u'',t)P_{\rm st}(u'). \tag{11}$$

The canonical formulation associates the conserved energy E (following from time translation invariance), the conserved momentum Π (from space translation invariance), and the conserved area M (from the Burgers equation with conserved noise):

$$E=\int dx\,\mathcal{H}, \tag{12}$$

$$\Pi=\int dx\,u\nabla p, \tag{13}$$

$$M=\int dx\,u. \tag{14}$$

The field equations (5) and (6) determine orbits in a canonical up phase space where the dynamical issue in determining S and thus P is to find an orbit from u' to u'' in time t. In general the orbits in phase space lie on the manifolds determined by the constants of motion E, Π, and M. Here the zero-energy manifold $E=0$ defines the stationary state. For vanishing or periodic boundary conditions the zero energy manifold is composed of the transient submanifolds $p=0$ and the stationary submanifold $p=2\nu u$. Generally, a finite energy orbit from $u'\to u''$ in time t migrates to the zero-energy manifold in the limit $t\to\infty$, yielding according to Eqs. (7) and (10) the stationary distribution $P_{\rm st}$

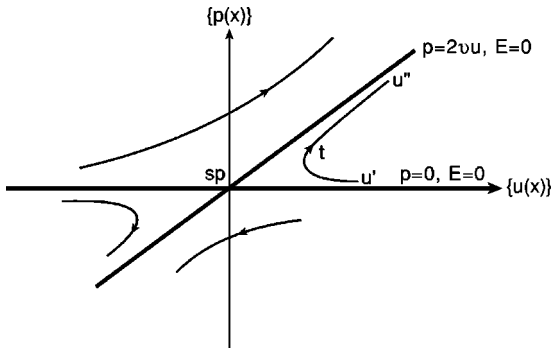

FIG. 1. We depict the generic behavior of the orbits in up phase space. The heavy lines indicate the transient zero-energy submanifold for $p=0$ and the stationary zero-energy submanifold for $p=2\nu u$. The stationary saddle point (sp) is at the origin. The finite time orbit from u' to u'' is attracted to the saddle point for $t\to\infty$.

$\propto\exp[-(\nu/\Delta)\int dx\,u^2]$ [30]. Finally, in the long time limit an orbit from $u'\to u''$ is attracted to the hyperbolic saddle point at the origin in phase space implying ergodic behavior in the stationary state. In Fig. 1 we have schematically depicted possible orbits in phase space.

The field equations (5) and (6) admit nonlinear soliton or smoothed shock wave solutions which are, in the static case, of kinklike form,

$$u_1(x)=u\tanh\left[\frac{\lambda|u|}{2\nu}x\right]. \tag{15}$$

Propagating solitons are subsequently generated by the Galilean boost (4). Denoting the right and left boundary values by u_+ and u_-, respectively, the propagation velocity is given by

$$u_++u_-=-2v/\lambda. \tag{16}$$

The amplitude of the static soliton is u and the soliton is located at the origin. The right hand soliton for $u>0$, i.e., the soliton with the larger right hand side boundary value, moves on the noiseless manifold $p=0$ and is also a solution of the damped (stable) noiseless Burgers equation for $\eta=0$. The noise-induced left hand soliton for $u<0$, i.e., the soliton with the larger left hand side boundary value, is associated with the noisy manifold $p=2\nu u$, and is a solution of the (unstable) noiseless Burgers equation with ν replaced by $-\nu$.

The heuristic physical picture that emerges from our analysis is that of a many body formulation of the pattern formation of a growing interface in terms of a dilute gas of propagating solitons matched according to the soliton condition (16). For illustration we have shown in Fig. 2 the slope field u, the corresponding height field h, and the noise field p for a four-soliton configuration.

In the present paper we embark on a numerical analysis of the coupled field equations (5) and (6) with the purpose of investigating them in more detail and provide a numerical underpinning of the heuristic quasiparticle picture advanced in the work referred to above. The paper is organized in the following manner. In Sec. II we discuss the soliton modes. In

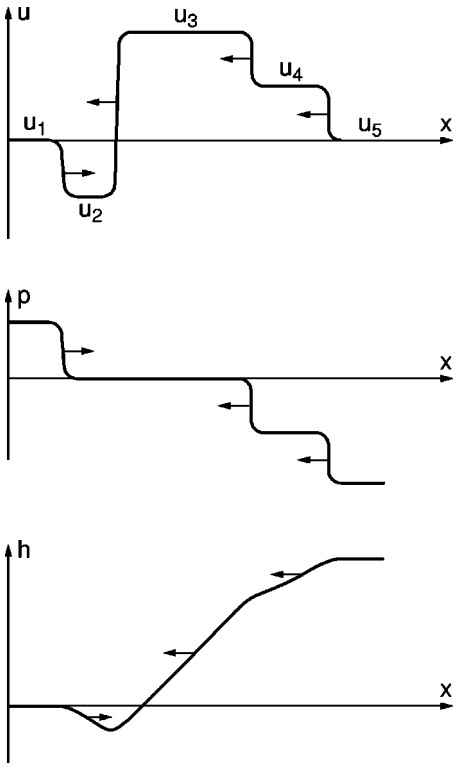

FIG. 2. We depict the four-soliton representation of the slope field u and noise field pa, and the associated height field h. The arrows indicate the propagation of the solitons.

Sec. III we introduce the numerical method designed to treat the inherent instability. In Sec. IV we present our numerical results for the scattering of two single solitons on a static soliton and the scattering of two soliton pairs. In Sec. V we discuss growth and anomalous diffusion associated with the modes investigated numerically. Section VI is devoted to a summary of our results and a conclusion.

II. SOLITON MODES

The exact right and left hand soliton solutions of the field equations do not satisfy periodic or vanishing boundary conditions in the slope field u; the nonvanishing boundary values u_+ and u_- in fact correspond to a deterministic current dissipated or generated at the soliton centers yielding permanent profile solutions [31]. The kink solitons constitute the elementary building blocks or ''quarks'' in the present approach and the interface profile is then built up by matching solitons according to the matching condition (16).

The simplest mode satisfying periodic boundary conditions is the two-soliton or pair soliton configuration

$$u_2(x,t)=u_1(x-vt-x_1)-u_1(x-vt-x_2), \qquad (17)$$

obtained by matching a right hand and a left hand soliton boosted to the velocity $v=-\lambda u$. The two-soliton mode has amplitude $2u$ and size $|x_2-x_1|$. The associated noise field vanishes for the right hand component and equals $2\nu u$ for the left hand component; we thus have

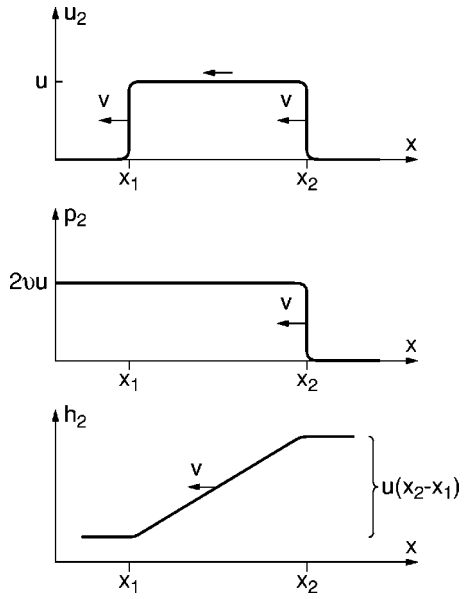

FIG. 3. We show the slope field u_2, the associated noise field p_2, and the resulting height profile h_2 at time $t=0$ for a two-soliton configuration. The arrows indicate the propagation of the solitons.

$$p_2(x,t)=\begin{cases}-2\nu u_1(x-vt-x_2) & \text{for} \quad u>0, \qquad (18)\\ +2\nu u_1(x-vt-x_1) & \text{for} \quad u<0. \qquad (19)\end{cases}$$

By inspection it is seen that the pair mode (17) is an approximate solution to the field equations (5) and (6). The correction terms are of the type $u\nabla u$ and $u\nabla p$ referring to the distinct components of u_2 and p_2 and thus correspond to local perturbations from a region of size $\nu/\lambda|u|$ which is small in the low viscosity limit $\nu\to 0$. We assume that the correction can be treated within a linear stability analysis and thus gives rise to a linear mode propagating between the right hand and left hand solitons [27].

The pair mode thus forms a long-lived excitation or quasiparticle in the many body description of a growing interface. Subject to periodic boundary conditions this mode corresponds to a simple growth situation. The propagation of the pair mode corresponds to the propagation of a step in the height field h. At each revolution of the pair mode the interface grows by a uniform layer of thickness $2u|x_2-x_1|$. In Fig. 3 we have depicted the pair mode in u, the associated noise field p, and the height profile h.

Generally a growing interface can at a given time instant be represented by a gas of matched left hand and right hand solitons as depicted in Fig. 2 in the four-soliton case. A gas of pair solitons thus constitutes a particular growth mode where the height profile between moving steps has horizontal segments. However, since we do not posses explicit propagating multisoliton solutions of the field equations (5) and (6) the problem of soliton collisions remains unresolved from an analytical point of view. Therefore we now turn to a numerical analysis of the problem.

III. NUMERICAL METHOD

The coupled field equations (5) and (6) are of the diffusion-advection type with the exception that the evolu-

tion of p is governed by a negative diffusion coefficient. Standard numerical methods designed to step the equations forward in time fail because small perturbations with wave number k grow in time as $\exp(\nu k^2 t)$, so perturbations with the largest possible k grow fastest, hence rendering the integration unstable. In order to circumvent this problem we have designed a method to solve the equations iteratively starting with a trial solution for u and p in the space interval $|x| \leqslant L$ and time interval $0 \leqslant t \leqslant T$. At each iteration step we proceed in two sweeps. In the forward sweep we step only the equation for u forward in time using $p(x,t)$ from the previous iteration step. In the backward sweep we step the equation for p backward in time, using $u(x,t)$ from the forward sweep. In this manner the unwanted perturbations in p decrease exponentially as one moves backward in time.

A drawback of this method is that we can specify initial values only for u, and that we must instead specify p at the final time $t=T$. In the present context where we want to consider collisions of solitons this is not a serious problem, because here it is possible to guess the final solution. The numerical solution serves therefore mainly as a tool to check that a certain guess is actually a solution. Furthermore, this method allows us to calculate the precise functional form of u and p during the collision, even if the initial guess around the time of the collision was actually wrong.

We have solved the equations on a mesh with $N_x = 1001$ mesh points and $N_t = 6001$ time steps. For $L = 1/2$ we have a mesh spacing of $\Delta x = 0.001$. For both sweeps we use sixth order finite differences to calculate first and second derivatives and a third order Runge-Kutta scheme for the time integration (see, e.g., the appendix of Ref. [32] for these schemes).

In order to adequately resolve u and p at all times we must choose a suitable value of ν. We found empirically that $\nu = 0.005$ gave good results, which is the value adopted in the following. For smaller values of ν the u and p functions become only marginally resolved whereas for larger values of ν the length of the time step is mostly controlled by the value of ν rather than just the propagation speeds of the solitons. Empirically we found that the maximum time step that can be used is $\Delta t = 5 \times 10^{-5}$ for $\nu = 0.005$. In all cases we have chosen $\lambda = 1$.

IV. SOLITONS, PAIR SOLITONS, AND SOLITON COLLISIONS

In choosing soliton configurations to be verified by the numerical method we have found that it is essential to satisfy the three conservation laws governing the dynamics of solitons, namely, the conservation of energy (12), the conservation of momentum (13), and the conservation of area (14).

A. Solitons and pair soliton

We have numerically verified that the right and left hand solitons (15) for $u > 0$ and $u < 0$ are solutions. By construction the two-soliton configuration (17) carries energy $E_2 = (-16/3)\lambda\nu|u|^3$, momentum $\Pi_2 = -4\nu u|u|$, and for small ν the area $M_2 \propto 2\nu|x_1 - x_2|$. We have shown that, for small ν, a well-separated two-soliton mode, i.e., with $|x_1 - x_2| \gg \nu/\lambda u$, is a long-lived excitation, hence justifying the heuristic argument.

In order to lend support to the heuristic quasiparticle picture based on the elementary kink solitons (quarks) and the composite pair soliton as the basic quasiparticle it is essential to consider soliton collisions. We have here considered the two symmetric cases: (i) the collision of two propagating solitons with a static soliton and (ii) the collision of two pair solitons. In both cases the configurations are symmetric and the conservation laws are satisfied at all times including the collision regime.

B. Three-soliton collisions

In the first case two propagating solitons moving in opposite directions collide with a static soliton located at the center. The trial solution has the form

$$u(x,t) = -\,\mathrm{sgn}(t)[u_1(x+vt) + u_1(x-vt) - 2u_1(2x)], \tag{20}$$

$$p(x,t) = \begin{cases} -2\nu[u_1(x+vt) + u_1(x-vt)] & \text{for } t<0 \quad (21) \\ -4\nu u_1(2x) & \text{for } t>0, \quad (22) \end{cases}$$

and the height field

$$h(x,t) = -\,\mathrm{sgn}(t)\left[\frac{2\nu}{\lambda}\right]\ln\left|\frac{\cosh[(\lambda|u|/2\nu)(x-vt)]\cosh[(\lambda|u|/2\nu)(x+vt)]}{\cosh[(\lambda|u|/2\nu)x]}\right| \tag{23}$$

with velocity $v = \lambda u$.

In this mode two left hand solitons with amplitude $2u$ propagate with equal and opposite velocities toward a static right hand soliton with amplitude $4u$ located at the center. During the collision the left hand solitons are absorbed, the static right hand soliton flips over to a static left hand soliton, and two right hand solitons emerge, propagating away from the center with equal and opposite velocity. The solitons thus collide transparently with the static soliton, i.e., there is no reflection, and there is no phase shift associated with the collision. In terms of the associated height profile this scattering situation corresponds to filling in a dip with subsequent nucleation of a growing tip.

Energy and momentum are associated with the noise-induced left hand solitons moving on the noisy manifold $p = 2\nu u$. By inspection of Eq. (20) it follows that the total

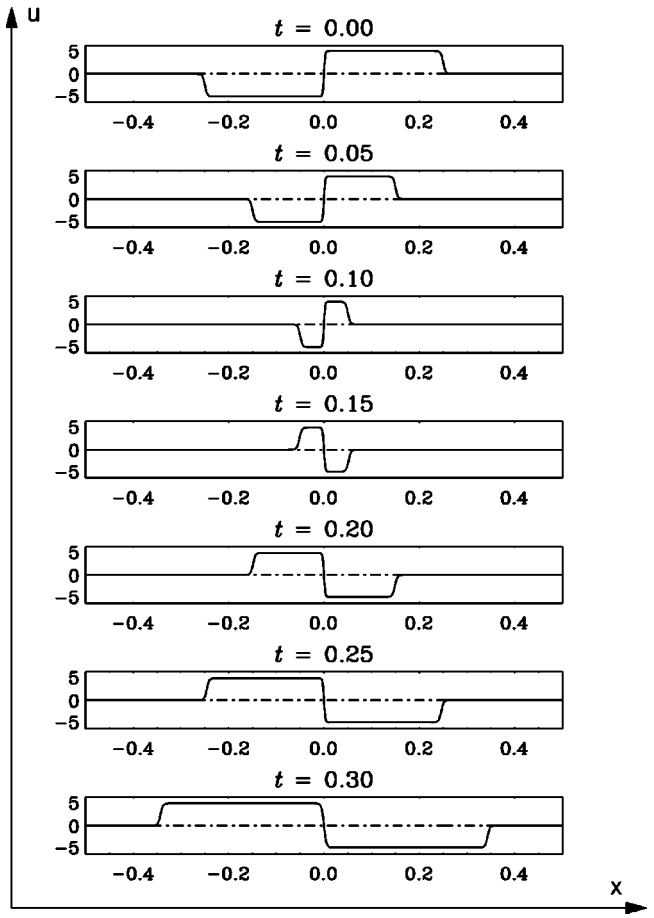

FIG. 4. Three-soliton collision: The slope field u as a function of x for different values of t.

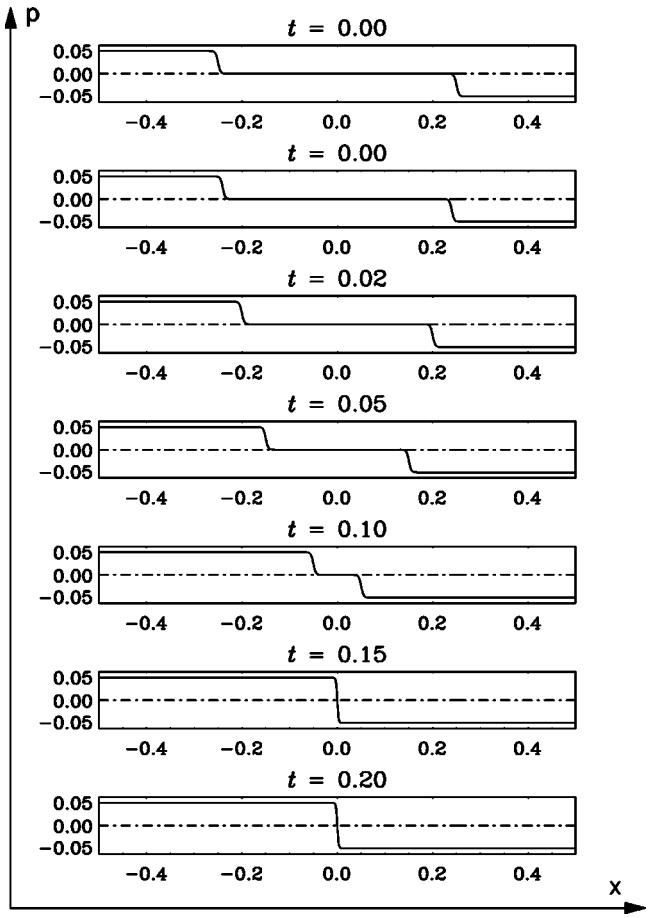

FIG. 5. Three-soliton collision: The noise field p as a function of x for the same values of t as in Fig. 4.

energy $E=-(32/3)\nu\lambda u^3$, the total momentum $\Pi=0$, and the total area $M=0$ are conserved during the collision.

Choosing the amplitude $u=2$ we have depicted in Fig. 4 the numerical verification of the slope field u as a function of x for different values of t. In Figs. 5 and 6 we show the associated noise field p and the height profile h as a function of x for the same values of t. In Fig. 7 we show a gray-scale representation of u in the xt plane. We notice that there is no phase shift associated with the scattering process.

C. Pair soliton collisions

In the second case we consider the collision of two pair solitons of equal size and amplitude. The trial solution propagating with velocity $v=\lambda u$ has the form

$$u(x,t)=-[u_1(x-vt+x_1)-u_1(x-vt+x_2)] +[u_1(x+vt-x_2)-u_1(x+vt-x_1)], \quad (24)$$

$$p(x,t)=-2\nu[u_1(x-vt+x_1)+u_1(x+vt-x_1)] \quad (25)$$

for $0<vt<x_2$,

$$u(x,t)=-[u_1(x-vt+x_1)-u_1(x)] +[u_1(x)-u_1(x+vt-x_1)], \quad (26)$$

$$p(x,t)=-2\nu[u_1(x-vt+x_1)+u_1(x+vt-x_1)] \quad (27)$$

for $x_2<vt<x_1$,

$$u(x,t)=+[u_1(x+vt-x_1)-u_1(x)] -[u_1(x)-u_1(x-vt+x_1)], \quad (28)$$

$$p(x,t)=-2\nu[u_1(x)+u_1(x)] \quad (29)$$

for $x_1<vt<2x_1-x_2$, and

$$u(x,t)=+[u_1(x+vt-x_1)-u_1(x+vt-2x_1+x_2)] -[u_1(x-vt+2x_1-x_2)-u_1(x-vt+x_1)], \quad (30)$$

$$p(x,t)=-2\nu[u_1(x+vt+2x_1-x_2)+u_1(x-vt+2x_1-x_2)] \quad (31)$$

for $2x_1-x_2<vt$.

In this mode two pair solitons of amplitude $2u$ propagate with equal and opposite velocities toward one another. The

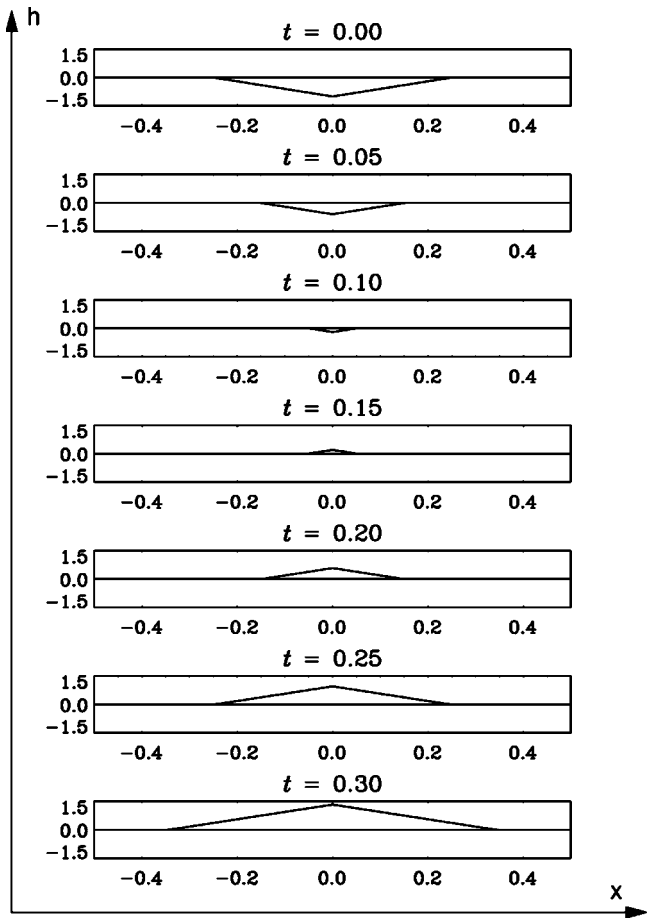

FIG. 6. Three-soliton collision: The height profile $h=\int u\,dx$ as a function of x for the same values of t as in Fig. 4.

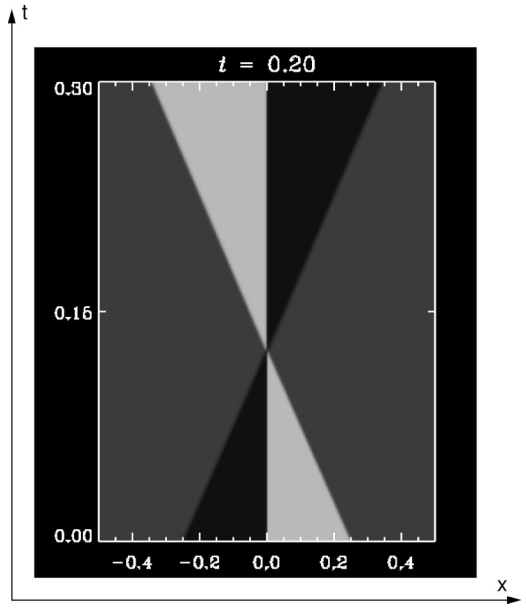

FIG. 7. Gray-scale representation of u in the xt plane showing the three-soliton collision. Note the absence of a phase shift during the collision.

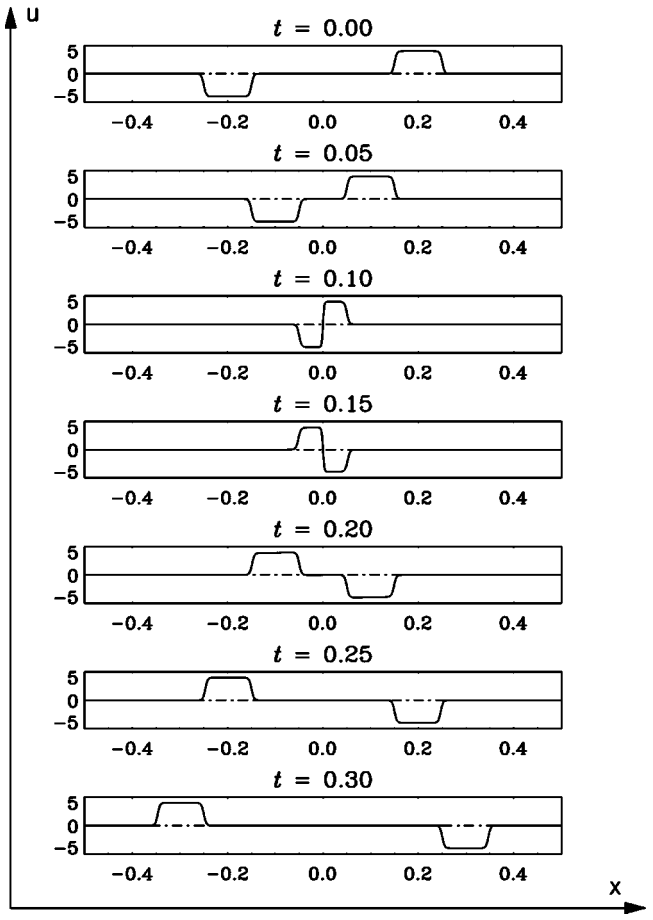

FIG. 8. Pair soliton collision: The slope field u as a function of x for different values of t.

two leading kink solitons merge to a static soliton and the two trailing kinks are absorbed. Subsequently, the static right hand soliton flips over to a static left hand soliton and the two pair solitons reemerge. Analyzing the collision, it follows that the scattering of pair solitons is transparent and accompanied by a phase shift in space equal to the soliton size $|x_2-x_1|$ or, equivalently, a time delay $|x_2-x_1|/v$. In terms of the associated height profile the scattering situation corresponds to filling in a trough due to two colliding steps and the subsequent nucleation of a growing plateau.

By inspection it again follows that the total energy $E=-(32/3)\nu\lambda u^3$, the total momentum $\Pi=0$, and the total area $M=0$ are conserved during collision.

Choosing the amplitude $2u$ and the kink positions $x_1=0.25$ and $x_2=0.15$ we show in Fig. 8 the numerical verification of the slope field u as a function of x for different values of t. In Figs. 9 and 10 we show the associated noise field p and the height profile h as a function of x for the same values of t. In Fig. 11 we show a gray-scale representation of u in the xt plane. We notice the phase shift engendered during the transparent collision.

V. GROWTH AND ANOMALOUS DIFFUSION

Since we have achieved numerical justification of three specific dynamical soliton configurations, namely, (i) the pair

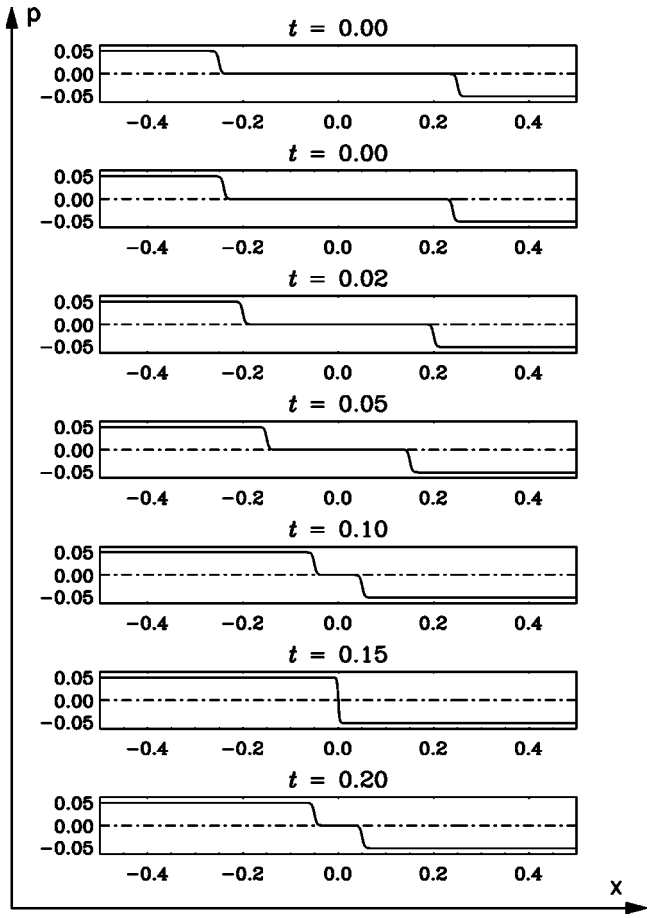

FIG. 9. Pair soliton collision: The noise field p as a function of x for the same values of t as in Fig. 8.

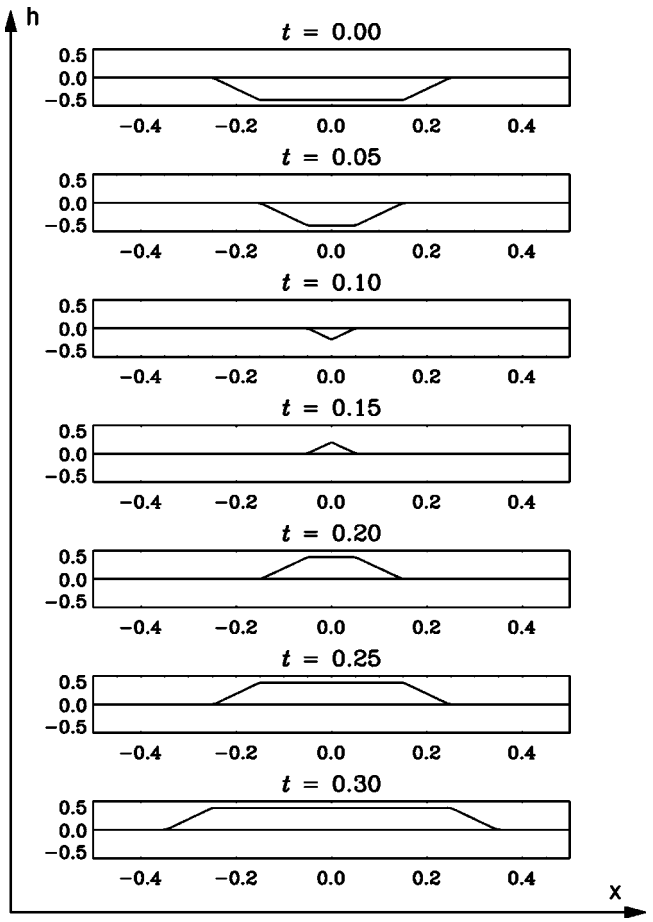

FIG. 10. Pair soliton collision: The height profile $h=\int u\,dx$ as a function of x for the same values of t as in Fig. 8.

soliton, (ii) the collision of two solitons with a static soliton, and (iii) the collision of two pair solitons, we can proceed to draw some simple conclusions based on the general framework discussed in Sec. I. There are two levels of description: the stochastic Langevin level and the deterministic Fokker-Planck or equation of motion level. On the Fokker-Planck level yielding the canonical field equations (5) and (6) the growth of the interface is interpreted in terms of a gas of propagating solitons (and diffusive modes). The stochastic description on the Langevin level is then established in the weak noise limit $\Delta\rightarrow 0$ by computing the action S associated with a particular dynamical mode and subsequently deduce the probability distribution according to Eq. (9), i.e., $P\propto\exp(-S/\Delta)$. This procedure is completely equivalent to the WKB limit of quantum mechanics. Here the wave function Φ and thus the probabilistic interpretation is given by $\Phi\propto\exp(iS/\hbar)$, where S is the action associated with the classical motion [28]. Note that unlike in quantum mechanics there is no phase interference in the stochastic nonequilibrium case. The long-lived pair soliton (17) has size $\ell=|x_1-x_2|$, amplitude $2u$, and propagates with velocity $v=-\lambda u$. During a revolution in a system of size L with periodic boundary conditions the height field increases with a layer of thickness $2u\ell$. Since the system is traversed in time $t=L/v$ the integrated growth velocity is given by $2\lambda u^2\ell/L$ which for a single pair of fixed size vanishes in the thermo-

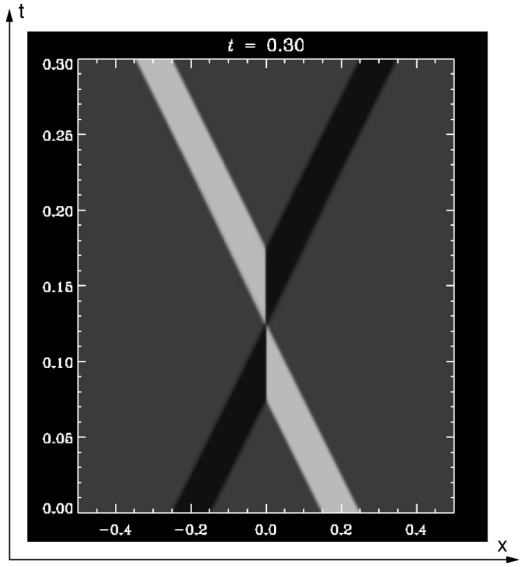

FIG. 11. Gray-scale representation of u in the xt plane showing the pair soliton collision. Note the occurrence of a phase shift during the collision.

dynamic limit. On the other hand, the local growth velocity dh/dt is given by $2\lambda u^2=(\lambda/2)(\nabla h)^2$ which is consistent with the averaged KPZ equation (3) in the stationary state.

The stochastic properties of the pair soliton growth mode is also easily elucidated by noting that the action associated with the pair mode is given by $S=(4/3)\nu\lambda|u|^3t$. Denoting the center of mass of the pair mode by $x=(x_1+x_2)/2$ we have $u=v/\lambda=x/t\lambda$ and we obtain using Eq. (9) the transition probability

$$P(x,t)\propto\exp\left(-\frac{4}{3}\frac{\nu}{\Delta\lambda^2}\frac{x^3}{t^2}\right) \tag{32}$$

for the ''random walk'' of independent pair solitons or steps in the height profile. Comparing Eq. (32) with the distribution for ''ordinary'' random walk originating from the Langevin equation $dx/dt=\eta,\langle\eta\eta\rangle(t)=\Delta\delta(t)$, $P(x,t)\propto\exp(-x^2/2\Delta t)$, we observe that the growth mode performs anomalous diffusion. The distribution (32) also implies the soliton mean square displacement, assuming pairs of the same average size,

$$\langle x^2\rangle(t)\propto\left(\frac{\Delta\lambda^2}{\nu}\right)^{1/z}t^{2/z}, \tag{33}$$

with dynamic exponent $z=3/2$, identical to the dynamic exponent defining the KPZ universality class. This result should be contrasted with the mean square displacement $\langle x^2\rangle\propto\Delta t^{2/z}$, $z=2$, for the ordinary random walk. The growth modes thus perform superdiffusion. We note that the distribution (32) is also obtained using the mapping of the KPZ equation to directed polymers in a random medium [5].

VI. SUMMARY AND CONCLUSION

In the present paper we have numerically investigated the coupled diffusion-advection type field equation originating from the canonical phase space approach applied to the noisy Burgers equation or the equivalent KPZ equation in one spatial dimension. We have shown that the pair soliton mode in the slope field corresponding to moving steps in the height field forms a long-lived excitation. We have furthermore investigated two special scattering scenarios, namely, the collision of two identical moving solitons with a static soliton and the collision of two identical pair solitons. They correspond in the height field, respectively, to the nucleation of a growing tip and the formation of a growing plateau. Finally, we have applied the canonical phase space approach in order to estimate the stochastic aspects following from the pair soliton mode propagation.

As discussed above the inherently unstable structure of the field equation makes a direct integration forward in time inaccessible and we thus cannot establish solutions as an initial value problem and discuss the equations generically. Consequently, we are limited to numerically check trial solutions representing a variety of scattering situations. So far we have been able to verify only the symmetric cases of three-soliton and soliton pair collisions. As a result we are also unable to address the issue of integrability or nonintegrability of the field equations. In order to extend the present numerical approach and thus provide substance to the heuristic quasiparticle representation of a growing interface, it is clearly of interest to design more involved trial solutions. Alternatively, a completely different approach to generate solutions is called for.

[1] D. Forster, D.R. Nelson, and M.J. Stephen, Phys. Rev. Lett. **36**, 867 (1976).
[2] D. Forster, D.R. Nelson, and M.J. Stephen, Phys. Rev. A **16**, 732 (1977).
[3] M. Kardar, G. Parisi, and Y.C. Zhang, Phys. Rev. Lett. **56**, 889 (1986).
[4] E. Medina, T. Hwa, M. Kardar, and Y.C. Zhang, Phys. Rev. A **39**, 3053 (1989).
[5] T. Halpin-Healy and Y.C. Zhang, Phys. Rep. **254**, 215 (1995).
[6] A. L. Barabasi and H. E. Stanley, *Fractal Concepts in Surface Growth* (Cambridge University Press, Cambridge, England, 1995).
[7] J. Krug, Adv. Phys. **46**, 139 (1997).
[8] E. Frey and U.C. Täuber, Phys. Rev. E **50**, 1024 (1994).
[9] E. Frey, U.C. Täuber, and T. Hwa, Phys. Rev. E **53**, 4424 (1996).
[10] E. Frey, U.C. Täuber, and H.K. Janssen, Europhys. Lett. **47**, 14 (1999).
[11] H. Janssen, U. Täuber, and E. Frey, Eur. Phys. J. B **9**, 491 (1999).
[12] M. Lässig, Phys. Rev. Lett. **80**, 2366 (1998).
[13] M. Lässig, Phys. Rev. Lett. **84**, 2618 (2000).
[14] F. Colaiori and M.A. Moore, Phys. Rev. Lett. **86**, 3946 (2001).
[15] F. Colaiori and M.A. Moore, Phys. Rev. E **63**, 057103 (2001).
[16] P.C. Martin, E.D. Siggia, and H.A. Rose, Phys. Rev. A **8**, 423 (1973).
[17] R. Bausch, H.K. Janssen, and H. Wagner, Z. Phys. B **24**, 113 (1976).
[18] H.C. Fogedby, Phys. Rev. E **57**, 4943 (1998).
[19] H.C. Fogedby, Phys. Rev. Lett. **80**, 1126 (1998).
[20] H.C. Fogedby, A.B. Eriksson, and L.V. Mikheev, Phys. Rev. Lett. **75**, 1883 (1995).
[21] M. I. Freidlin and A. D. Wentzel, *Random Perturbations of Dynamical Systems* (Springer-Verlag, New York, 1984).
[22] R. Graham and T. Tél, J. Stat. Phys. **35**, 729 (1984).
[23] R. Graham, *Noise in Nonlinear Dynamical Systems, Vol. 1, Theory of Continuous Fokker-Planck Systems*, edited by F. Moss and P. E. V. McClintock (Cambridge University Press, Cambridge, England, 1989).
[24] H.C. Fogedby, Phys. Rev. E **59**, 5065 (1999).
[25] H.C. Fogedby, Phys. Rev. E **60**, 4950 (1999).
[26] H.C. Fogedby, Europhys. Lett. **56**, 492 (2001).

[27] H.C. Fogedby, Eur. Phys. J. B **20**, 153 (2001).
[28] L. Landau and E. Lifshitz, *Quantum Mechanics* (Pergamon Press, Oxford, 1959).
[29] L. Landau and E. Lifshitz, *Mechanics* (Pergamon Press, Oxford, 1959).
[30] D.A. Huse, C.L. Henley, and D.S. Fisher, Phys. Rev. Lett. **55**, 2924 (1985).
[31] H.C. Fogedby, Phys. Rev. E **57**, 2331 (1998).
[32] F.J. Sánchez-Salcedo and A. Brandenburg, Mon. Not. R. Astron. Soc. **322**, 67 (2001).